Cell Reports
Medicine

Article

Phase 1 clinical trial to assess safety and efficacy of NY-ESO-1-specific TCR T cells in HLA-A*02:01 patients with advanced soft tissue sarcoma

Graphical abstract

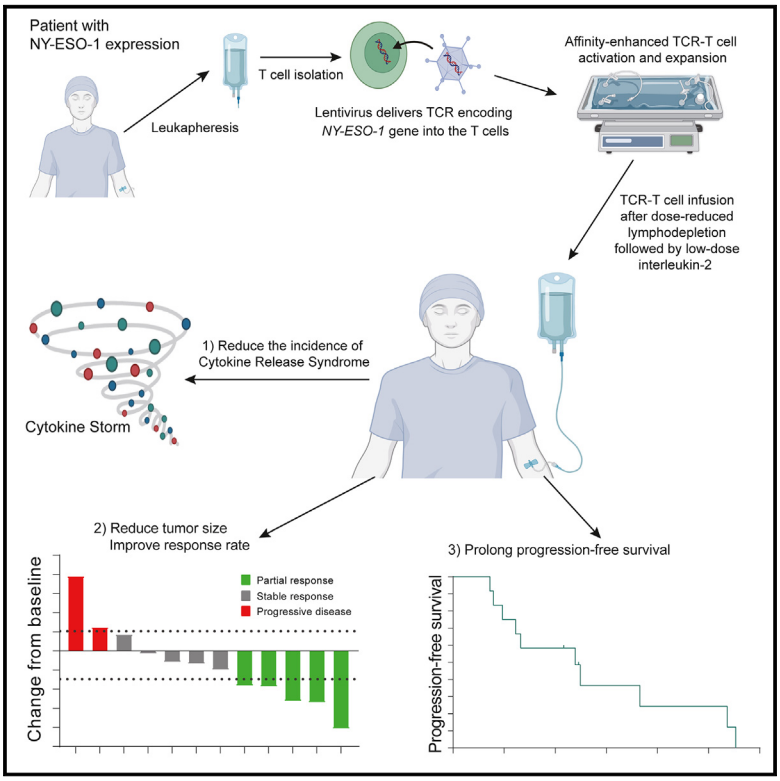

Highlights

- TAEST16001 cells are high-affinity NY-ESO-1-specific TCR-T cells
- TAEST16001 cell therapy is well tolerated in advanced soft tissue sarcoma
- TAEST16001 cell therapy has promising anti-tumor activity and durable response
- Several prespecified biomarkers are associated with patient response

Authors

Qiuzhong Pan, Desheng Weng, Jiayong Liu, ..., Yi Li, Zhengfu Fan, Xing Zhang

Correspondence

li_yi@gibh.ac.cn (Y.L.), zhengfufan@126.com (Z.F.), zhangxing@sysucc.org.cn (X.Z.)

In brief

Pan et al. demonstrate the safety, efficacy, and survival of TAEST16001 cells in HLA-A*02:01 patients with advanced soft tissue sarcoma. They show that TAEST16001 cell therapy is well tolerated and has promising anti-tumor activities for advanced soft tissue sarcoma expressing the NY-ESO-1 antigen.

Pan et al., 2023, Cell Reports Medicine *4*, 101133
August 15, 2023
https://doi.org/10.1016/j.xcrm.2023.101133

CellPress

Cell Reports Medicine

CellPress
OPEN ACCESS

Article

Phase 1 clinical trial to assess safety and efficacy of NY-ESO-1-specific TCR T cells in HLA-A*02:01 patients with advanced soft tissue sarcoma

Qiuzhong Pan,[1,6] Desheng Weng,[1,6] Jiayong Liu,[2,6] Zhaosheng Han,[3,6] Yusheng Ou,[3] Bushu Xu,[1] Ruiqing Peng,[1] Yi Que,[1] Xizhi Wen,[1] Jing Yang,[1] Shi Zhong,[3] Lun Zeng,[3] Aiyuan Chen,[3] Haiping Gong,[3] Yanmei Lin,[3] Jiewen Chen,[3] Ke Ma,[3] Johnson Y.N. Lau,[4,5] Yi Li,[3,*] Zhengfu Fan,[2,*] and Xing Zhang[1,7,*]

[1]Melanoma and Sarcoma Medical Oncology Unit, State Key Laboratory of Oncology in South China, Sun Yat-sen University Cancer Center, Guangzhou 510060, P.R. China

[2]Key Laboratory of Carcinogenesis and Translational Research (Ministry of Education/Beijing), Department of Bone and Soft Tissue Tumor, Peking University Cancer Hospital & Institute, 52 Fucheng Road, Beijing 100142, P.R. China

[3]Xiangxue Life Science Technology (Guangdong) Co., Ltd., Guangzhou 510663, P.R. China

[4]Axis Therapeutics, Ltd., Hong Kong SAR, P.R. China

[5]Athenex, Conventus Building, 1001 Main Street, Suite 600, Buffalo, NY 14203, USA

[6]These authors contributed equally

[7]Lead contact

*Correspondence: li_yi@gibh.ac.cn (Y.L.), zhengfufan@126.com (Z.F.), zhangxing@sysucc.org.cn (X.Z.)

https://doi.org/10.1016/j.xcrm.2023.101133

SUMMARY

New York esophageal squamous cell carcinoma-1 (NY-ESO-1)-specific T cell receptor (TCR) T cell therapy is effective in tumors with NY-ESO-1 expression, but a safe and effective TCR-T cell therapeutic protocol remains to be improved. Here, we report a phase 1 investigational new drug clinical trial with TCR affinity-enhanced specific T cell therapy (TAEST16001) for targeting NY-ESO-1. Enrolled patients receive TAEST16001 cell infusion after dose-reduced lymphodepletion with cyclophosphamide (15 mg/kg/day × 3 days) combined with fludarabine (20 mg/m^2/day × 3 days), and the TCR-T cells are maintained with low doses of interleukin-2 injection post-adoptive transfer. Analysis of 12 patients treated with the regimen demonstrates no treatment-related serious adverse events. The overall response rate is 41.7%. The median progression-free survival is 7.2 months, and the median duration of response is 13.1 months. The protocol of TAEST16001 cells delivers a safe and highly effective treatment for patients with advanced soft tissue sarcoma (ClinicalTrials.gov: NCT04318964).

INTRODUCTION

Soft tissue sarcomas (STSs) are a group of heterogeneous mesenchymal cancers that comprise more than 50 different histological types.[1] About 60% of patients with STS present with localized disease at the time of diagnosis, and 40% of patients develop metastases within 5 years.[2] Treatment options for advanced, unresectable, or metastatic STS are scarce, both in number and efficacy. Anthracycline (e.g., doxorubicin), either as monotherapy or in combination with ifosfamide, is the most conventional first-line treatment regimen.[3] After progression on an anthracycline regimen, second-line treatment options include dacarbazine, ifosfamide, gemcitabine, docetaxel, trabectedin, eribulin, or pazopanib.[1,4] However, survival benefits with these drugs are generally unsatisfactory because they are correlated with low overall response rates (5%–16%), short duration of disease control, and risk of treatment-related side effects.[5] Thus, there is an urgent need for more effective and tolerable treatment for patients with advanced STS, and immunotherapy may offer attractive solutions.

Immunotherapy with immune checkpoint inhibitors represents a landscape for the management of many solid tumors. However, the total objective response rate (ORR) of anti-PD-1 antibody monotherapy in sarcomas was only 5%–18%,[6,7] which is far from fulfilling clinical demand. Moreover, the progression-free survival (PFS) and overall survival (OS) data of the current immune checkpoint inhibitor trials were similar to that of traditional chemotherapy trials in sarcomas.[8] Poor T cell infiltration, marginal PD-L1 expression, and lower levels of nonsynonymous somatic mutation burden in sarcoma may at least partially explain the poor clinical benefit of immune checkpoint inhibitors.[9,10] Therefore, other immunotherapy approaches, such as adoptive T cell immunotherapy, deserve important exploration in sarcomas.

New York esophageal squamous cell carcinoma-1 (NY-ESO-1) is a cancer-germline antigen (CGA) or cancer-testis antigen that is expressed in a wide range of tumor types.[11] NY-ESO-1 has been considered a potential target of immunotherapy in sarcomas[12] and is reported to be expressed in 88% of myxoid liposarcomas, 49% of synovial sarcomas, and 35% of myxofibrosarcomas by immunohistochemical staining.[13] Although several previous studies have demonstrated that adoptively transferred patient-derived T cell receptor (TCR)-engineered

T cells (TCR-T) specific for NY-ESO-1 are preliminarily effective in NY-ESO-1$^+$ synovial sarcomas,[14–18] some important questions of TCR-T cell therapy such as the consensus on optimal affinity, cell dose, predictive biomarkers, and minimized toxicity still needed to be explored.

T cell infiltration is required for effective T cell therapy. TCR-T cell tumor infiltration can be improved by optimizing the TCR-pHLA interation.[19] This improvement can be achieved by generating high-affinity TCR through mutations in complementarity-determining regions (CDRs).[19] Using previously published approaches,[20,21] we enhanced the affinity of a TCR, which was isolated with previously published methods[22] from peripheral blood mononuclear cells (PBMCs) of a healthy donor, by phage display for the development of TCR-engineered T cells (TAEST16001 cells) specific for the NY-ESO-1$_{157–165}$ epitope in complex with HLA-A*02:01. Our preclinical investigation indicated a good safety and efficacy for TAEST16001 cells (data not shown). Here, we report results from an open-label, dose-escalating phase 1 investigational new drug clinical trial evaluating safety, tolerability, pharmacokinetics, pharmacodynamics, and preliminary efficacy of TAEST16001 cells maintained with low-dose interleukin-2 (IL-2) in patients after dose-reduced lymphodepletion for the treatment of advanced soft tissue sarcoma. We also investigated the correlations between responses and selected prespecified biomarkers.

RESULTS

Manufacturing of TAEST16001 cells

We developed a manufacturing procedure for producing TCR-T cells under good manufacturing practice (GMP) conditions using closed and semi-closed modular systems (Figure S1A). To validate the procedure, TAEST16001 cells were produced using PMBCs from three healthy donors. The final products showed a predominant memory phenotype (Figure S1B) and mediated interferon γ (INF-γ) release and specific lysis of NY-ESO-1$^+$ tumor cell lines or T2 cells loaded with the NY-ESO-1$_{157–165}$ peptide (Figures S1C–S1G). The manufacturing procedure was used for all the patients in this clinical study.

Patient and treatment characteristics

Between March 23, 2020, and December 31, 2021, 436 patients with sarcoma were screened for HLA-A*02:01 and NY-ESO-1 expression. A total of 12 HLA-A*02:01$^+$ patients with NY-ESO-1$^+$ advanced, unresectable sarcoma were included (Figure S2). Of the 12 enrolled patients, 10 had synovial sarcomas and 2 had liposarcomas (1 myxoid liposarcoma, 1 dedifferentiated liposarcoma). The median age was 33 (25–67) years, and 58.3% (7/12) of patients were men. 83.3% of patients had received at least 2 lines of prior chemotherapy. The median time from enrollment to TAEST16001 cell infusion was 43 days (interquartile range [IQR], 35.5–46.5 days). All 12 patients received modified lymphodepletion, which was a lower dose of precondition than previously reported (Table S1),[14,15,17] followed by a median of 3.24×10^9 TAEST16001 cells (range, $0.51–11.96 \times 10^9$) plus low-dose systemic IL-2 (500,000 IU per time, twice daily for 14 days). Characteristics of the patients and the administered TCR-T cells are shown in Tables 1 and S2, respectively.

Safety and tolerability of TAEST16001 cells

No predefined dose-limiting toxicities (DLTs) within 28 days after TAEST16001 cell infusion were observed during the dose-escalation phase. The most common adverse events of grade 3 or higher among the 12 treated subjects were lymphopenia (100%), neutropenia (92%), leukopenia (83%), and anemia (33%), which were primarily attributable to the precondition of lymphodepletion (Table 2). Other relevant grade 3–4 toxicities included fever (8%), thrombocytopenia (8%), hypokalemia (8%), increased alanine aminotransferase (8%), proteinuria (8%), and hypertriglyceridemia (8%). Two patients in the second cell-dose level experienced grade 2 cytokine release syndrome (CRS) and developed fever on the second day after the cell infusion. Hypotension and hypoxia occurred in the two patients on the third and fourth days, respectively. One patient was treated with tocilizumab, the other with oxygen therapy, and both recovered from CRS within 1 week with no remaining complications. None of the patients had neurotoxicity or serious adverse events related to cell infusion.

Efficacy of TAEST16001 cells

All 12 patients that received the prescribed cell dose of TAEST16001 were eligible for efficacy analysis, and 9 (75%) patients showed tumor regression (Figure 1A). Patients infused with TAEST16001 cells in this trial demonstrated a median time to response (TTR) of 1.9 months (range, 0.9–3 months) and a median duration of response of 13.1 months (range, 5–14.3 months; Figures 1B and S3). Six (50%) patients experienced continued decreases in tumor burden following the first radiological assessment (Figure 1C). At the time of the primary analysis, the best response was partial response in 5 of 12 patients for an ORR of 41.7% (95% confidence interval [CI], 15.2–72.3; Figure 1A; Table S3). Five (41.7% [95% CI, 15.2–72.3]) patients achieved stable disease for a disease control rate of 83.3% (95% CI, 51.6–97.9). Four of five (80%) patients without lung metastases had partial response. The median PFS was 7.2 months (95% CI, 2.5–11.8) (Figure 1D). At the time of data cutoff (April 15, 2022), 10 patients had disease progression, and one of them had died from disease. Therefore, the proportion censored at the time was 11/12 (91.7%), and the median OS was immature.

Notably, patient T06 (42-year-old male), who had received two prior lines of therapy and experienced grade 2 CRS after TAEST16001 treatment, exhibited a partial response of upper arm and multiple lung metastatic lesions after 4 weeks of cell infusion, maintaining more than 14 months following treatment (Figure 2A). As the lung metastatic lesions remained a great partial response even at the time of progression, the patient underwent surgical resection of a lesion in the upper arm. Another patient, T02 (27-year-old male), who had recurrent myxoid liposarcoma in the right leg after receiving five surgeries, also exhibited a partial response and sustained more than 1 year following treatment (Figure 2B).

TAEST16001 cell expansion and persistence

All 12 patients were assessed for pharmacokinetics. The TCR gene copies per μg genomic DNA (gDNA) at prescribed points before and after infusion are shown in Figure 3A. The median C_{max} value after cell infusion was 52,582 copies per μg gDNA

Table 1. Baseline characteristics of patients

Patient	Age (years)	Gender	Sites of disease	Prior chemotherapy regimens[a]	Pathological subtype	NY-ESO-1 expression (%)	Cells ($\times 10^9$)
T01	67	M	leg	2: doxorubicin+ifosfamide+ dacarbazine, apatinib	synovial sarcoma	70	0.53
T02	27	M	leg	1: doxorubicin+ifosfamide	myxoid liposarcoma	90	0.51
T03	40	M	arm, pleura, mediastinum	3: doxorubicin+ifosfamide, anlotinib+TQB2450 (clinical trial), apatinib	synovial sarcoma	100	0.51
T04	28	F	arm, pleura, lung	3: cyclophosphamide+ epirubicin+vindesine+ dacarbazine, apatinib, pazopanib	synovial sarcoma	100	1.94
T05	25	F	lung, vertebra, mediastinum	2: doxorubicin+ifosfamide, anlotinib	synovial sarcoma	90	1.70
T06	42	M	arm, lung	2: doxorubicin+ifosfamide, anlotinib	synovial sarcoma	30	1.86
T07	33	M	leg, lung	2: doxorubicin+ifosfamide, ifosfamide	synovial sarcoma	95	4.65
T08	37	F	arm, lung, pleura	2: doxorubicin+ifosfamide, ifosfamide	synovial sarcoma	95	4.71
T09	33	M	arm, lung	2: doxorubicin+ifosfamide, ifosfamide	synovial sarcoma	35	4.55
T10	32	M	leg, lung, pleura, bone	3: doxorubicin+ifosfamide+ dacarbazine+endostar, doxorubicin+dacarbazine+ endostar+anti-PD-1 antibody, anlotinib	synovial sarcoma	40	11.09
T11	64	F	arm	1: doxorubicin+ifosfamide	dedifferentiated liposarcoma	40	11.96
T12	27	F	subcutaneous, liver, peritoneum, pelvis	2: gemcitabine+docetaxel, doxorubicin+ifosfamide	synovial sarcoma	95	9.56

F, female; M, male.
[a]Lines of therapy: names of agents.

(range, 11,156–838,655), and the median T_{max} value was 6 days (range, 0.08–20). The C_{max} value did not show significant differences among the four dosing groups (Figure 3B). There was a trend toward increased expansion of the TCR-T cells as assessed by qPCR in the responders (median, 103,806 copies per μg gDNA; range, 26,260–838,655) compared with the nonresponders (median, 25,160 copies per μg gDNA; range, 11,156–447,847; Figure 3C, p = 0.1061). Circulating TCR-expressing T cells were detected in the 5 patients for whom monitoring continued beyond 25 weeks (Figure 3A).

Phenotypic evolution of TAEST16001 cells over time

The memory cell phenotype of the TAEST16001 cells was assessed in the manufactured product and following infusion in a subset of patients. We evaluated the following four T cell subsets, naive T (T_N; $CD45RO^-CCR7^+$) cells, central memory T (T_{CM}; $CD45RO^+CCR7^+$) cells, effector memory T (T_{EM}; $CD45RO^+CCR7^-$) cells, and terminally differentiated effector T (T_{TE}; $CD45RO^-CCR7^-$) cells and found that T_N was the lowest proportions in the four T cell subsets in the manufactured product (p = 0.0335; Figure 4A). After adoptive transfer, we consistently observed an increase in the frequency of T_{CM} and T_{EM} subsets within the circulating $Tetramer^+$ $CD3^+$ TCR-T cells (Figures 4A and 4B). The increase of the frequency of T_{CM} (p = 0.0365) and T_{EM} (p = 0.0268) subsets was more significantly obvious on days 180–270 after cell infusion (Figure 4A). We also analyzed the correlation between frequencies of T cell subsets in the manufactured product and the peak of TCR gene copies per μg gDNA after cell infusion. The results revealed that the frequency of $CD45RO^+CCR7^-$ (T_{EM}) cells was positively correlated with the peak of TCR gene copies per μg gDNA (Figure 4C).

Correlation between peripheral blood biomarkers and response

Several kinds of inflammatory cytokines, including IL-2, IL-6, IL-10, IFN-γ, serum amyloid A (SAA), C-reactive protein (CRP), and ferritin, as well as the phenotype of peripheral blood T cells, were detected after cell infusion. We found that the median (range) times of the peak value for IL-2, IL-6, IL-10, IFN-γ, SAA, CRP, and ferritin were 2 (1–19), 3 (2–6), 3.5 (2–9), 3 (1–7), 5 (3–20), 4.5 (3–6), and 6 days (3–9), respectively. No statistically significantly correlation was found between response and peak value of IL-2, IL-6, IL-10, SAA, and ferritin. However, the peak values of IFN-γ (p = 0.0051) as well as CRP (p = 0.0303) were statistically

Table 2. Adverse events

Adverse event	Grade 1 (%)	Grade 2 (%)	Grade 3 (%)	Grade 4 (%)	Total (%)
Hematological					
Neutropenia	0 (0)	1 (8)	5 (42)	6 (50)	12 (100)
Lymphopenia	0 (0)	0 (0)	1 (8)	11 (92)	12 (100)
Leukopenia	0 (0)	2 (17)	4 (33)	6 (50)	12 (100)
Anemia	3 (25)	3 (25)	4 (33)	0 (0)	10 (83)
Thrombocytopenia	2 (17)	0 (0)	1 (8)	0 (0)	3 (25)
Metabolism and nutrition disorders					
Hypoalbuminemia	10 (83)	2 (17)	0 (0)	0 (0)	12 (100)
Hypocalcemia	5 (42)	6 (50)	0 (0)	0 (0)	11 (92)
Hyponatremia	8 (67)	1 (8)	0 (0)	0 (0)	9 (75)
Hyperglycemia	7 (58)	1 (8)	0 (0)	0 (0)	8 (67)
Hypokalemia	5 (42)	1 (8)	1 (8)	0 (0)	7 (58)
Decreased appetite	5 (42)	2 (17)	0 (0)	0 (0)	7 (58)
Gastrointestinal					
Constipate	3 (25)	3 (25)	0 (0)	0 (0)	6 (50)
Diarrhea	3 (25)	3 (25)	0 (0)	0 (0)	6 (50)
Nausea	4 (33)	2 (17)	0 (0)	0 (0)	6 (50)
Vomit	4 (33)	2 (17)	0 (0)	0 (0)	6 (50)
Other					
Fever	4 (33)	7 (58)	1 (8)	0 (0)	12 (100)
Increased ALT	7 (58)	0 (0)	1 (8)	0 (0)	8 (67)
Proteinuria	5 (42)	1 (8)	1 (8)	0 (0)	7 (58)
Fatigue	7 (58)	0 (0)	0 (0)	0 (0)	7 (58)
Hypertriglyceridemia	4 (33)	1 (8)	1 (8)	0 (0)	6 (50)
Increased AST	3 (25)	2 (17)	0 (0)	0 (0)	5 (42)
Chills	4 (33)	1 (8)	0 (0)	0 (0)	5 (42)
Dizziness	4 (33)	0 (0)	0 (0)	0 (0)	4 (33)
Cytokine release syndrome	0 (0)	2 (17)	0 (0)	0 (0)	2 (17)
Neurotoxicities	0 (0)	0 (0)	0 (0)	0 (0)	0 (0)

ALT, alanine aminotransferase; AST, aspartate aminotransferase.

significantly higher in responders than those in nonresponders (Figure 5). Accordingly, the percentage of $CXCR3^+CD3^+$ T cells or $CXCR3^+CD3^+CD8^+$ T cells on day 28 after cell infusion were significantly positively correlated with patient responses (Figure S4). Other T cell subsets, such as $CD3^+CD4^+$, $CD3^+CD8^+$, T_N, T_{CM}, T_{EM}, T_{TE}, $CD3^+CD25^+Foxp3^+$ (regulatory T [Treg] cells), $CD3^+CXCR6^+$, $CD3^+PD\text{-}1^+$, $CD3^+LAG\text{-}3^+$, $CD3^+TIM\text{-}3^+$, $CD3^+CTLA4^+$, $CD3^+CD8^+CXCR6^+$, $CD3^+CD8^+PD\text{-}1^+$, $CD3^+CD8^+LAG\text{-}3^+$, $CD3^+CD8^+TIM\text{-}3^+$, and $CD3^+CD8^+CTLA4^+$, were unrelated to patient responses (Figure S4).

DISCUSSION

Adoptive T cell therapy with HLA-A*02:01-restricted NY-ESO-1-transduced T cells has shown promising results in patients with NY-ESO-1 antigen expression.[14–18] However, the safety and effectiveness of NY-ESO-1-specific TCR-T cell therapy remain to be further optimized. In our previous study, we developed NY-ESO-1-specific TCR-T cells (TAEST16001 cells), of which the TCR was affinity enhanced by phage display from a parental TCR isolated from PBMCs of an HLA-matched healthy donor (data not shown), differing from the popular TCR that was affinity enhanced by random mutations from a 1G4 TCR isolated from a patient with cancer.[17,23] TAEST16001 cells showed good specificity and safety in previous investigator-initiated trial (data not shown; ClinicalTrials.gov: NCT03462316). Therefore, in the current phase 1 study, we further evaluated the safety and clinical activity of TAEST16001 cells in HLA-A*02:01-positive patients with advanced soft tissue sarcomas expressing the NY-ESO-1 antigen.

By this rigorous dose-escalation study, we further demonstrated that TAEST16001 cell treatment was well tolerated in terms of no serious adverse events related to cell infusion and no treatment-related deaths or adverse events leading to study withdrawal, although the maximum escalating dose of TAEST16001 cells in the study was lower than the dose already used in the National Cancer Institute studies.[15] Besides, our results suggested that the maximum escalating dose in this study, which tended to correlate with increased expansion level of TCR-T cells *in vivo* and have similar safety with the low-level

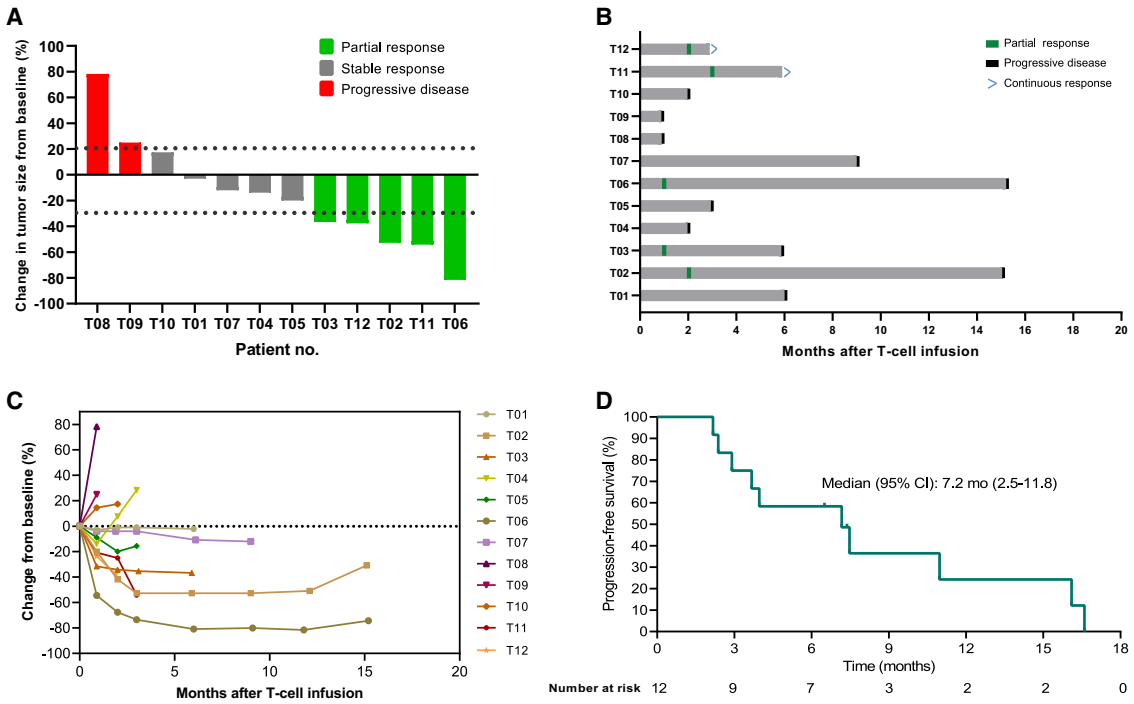

Figure 1. Clinical response and progression-free survival outcomes in 12 patients who were treated with TAEST16001 cells

(A) Waterfall plot of the best clinical response for each evaluable patient.

(B) Swimlane plot shows clinical outcomes of treated patients.

(C) Spider plot shows the change in the sum of the diameters of each patient's target lesions over time.

(D) Kaplan-Meier estimates of the progression-free survival. Tick marks indicate the time of data censoring at their last date of contact.

dose, could be selected for dose confirmation in phase 2 study. Once the maximum escalating dose was determined to be safe and effective, a higher cell dose beyond the maximum escalating dose may be unnecessary in patient treatment for cost-effective reasons.

Another aspect of good tolerance is manifested by the grade 4 adverse events and adverse events of special interest (CRS and neurotoxicity). No grade 4 adverse events other than hematological toxicity occurred. The incidence and grade of CRS reported in our study (16.7%, 2/12) were both lower than that observed in a previous study of NY-ESO-1-specific TCR-T cell therapy (41.6%, 5/12).[14] The differences in the incidence and severity of CRS between ours and others may be partially related to lymphodepletion intensity and IL-2 dose (Table S1). Previous TCR-T trials administered a lymphodepletion regimen containing a high dose of fludarabine with cyclophosphamide to support TCR-T cell engraftment and improve clinical efficacy (Table S1).[14–17] Our lymphodepleting regimen utilized dose-reduced fludarabine (60 mg/m^2) and cyclophosphamide (45 mg/kg). Besides, instead of high-dose IL-2, such as 720,000 IU/kg three times daily,[15,17] low-dose IL-2 (500,000 IU, twice daily for 14 days) was used after cell infusion in our study, which is even lower than the low-dose IL-2 (500,000 IU/m^2 twice daily for 14–28 days) used in another clinical study.[24] Modified (dose-reduced) lymphodepletion with fludarabine and cyclophosphamide and low-dose IL-2 usage may contribute to the moderate adverse events observed in our clinical study. In addition, the affinity of TCR is considered to be related to the toxicity of TCR-T cell therapy.[25,26] Severe lung injury or lethal cardiotoxicity has been reported in several studies related to affinity-enhanced TCR-T cells.[18,24,27] However, our NY-ESO-1-specific TCR with optimal affinity and specificity was selected with phage display libraries, which were constructed on templates of a TCR from a health donor, and the affinity-enhancement approaches were verified to maintain good antigen specificity and potentially enlarge therapeutic windows.[28] Unlike the high incidence of immune effector cell-associated neurotoxicity syndrome (ICANS) in chimeric antigen receptor (CAR) T cells treatment,[29] no neurotoxicity was observed in our study. This may relate to the TCR-T and CAR-T forming different immunologic synapses.[30] Collectively, these data provided evidence that TAEST16001 cell treatment was safe when used with modified lymphodepletion and low-dose IL-2.

The impressive responses to TAEST16001 cells included a median TTR of 1.9 months and 41.7% ORR, indicating highly efficient anti-tumor activity by TAEST16001 cells. The median PFS was 7.2 months, and a median OS was not reached. As observed in previous studies,[14,17] not all patients respond to TCR-T cell therapy. Low expansion peak of TCR-T cells in peripheral blood, downregulation of HLA, and defects in the antigen-presenting machinery may explain the primary resistance to TCR-T cell therapy.[31] Although cross-study comparisons have limitations, the response rate, time, and durability are comparable to the previous NY-ESO-1-specific TCR-T cell trial reported by D'Angelo et al., in

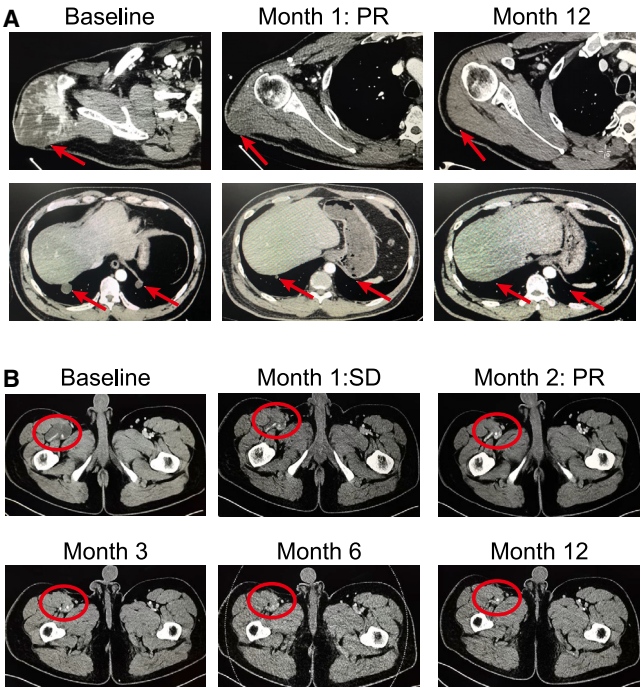

Figure 2. Computed tomography (CT) scans demonstrating tumor regression

(A) CT scans from patient T06, who had large synovial sarcoma in the right arm with numerous lung metastatic lesions.

(B) CT scans from patient T02, who had recurrent myxoliposarcoma in the right leg. Red arrows and ellipse point to tumors.

which the ORR was 50%, the TTR was 6.2 weeks, and the median PFS was 15 weeks.[14] It is reported that T cells equipped with a high-affinity TCR exhibited increased anti-tumor effects because of their improvement of intratumor infiltration[23] and faster and better response to antigen recognition.[17,32] Another two clinical trials also reported a high ORR in patients with synovial sarcoma after NY-ESO-1-specific TCR-T cell infusion.[15,17] As stated above, a high dose of fludarabine with cyclophosphamide and high-dose IL-2 were used in their studies,[15,17] which might be related to the high ORR. In fact, a majority of patients eventually exhibited progressive disease after a period of remission in all these studies. A possible reason for patients' resistance to TCR-T cell therapy may be related to T cell exhaustion after overactivation of high-affinity TCR-T cells,[25,26,33] as exhausted T cells show progressive loss of anti-tumor function and upregulate the expression of inhibitory receptors.[34] Further studies are needed for a better understanding of the mechanisms underlying acquired resistance against TCR-T cells.

Excitedly, two patients with liposarcoma had objective responses in the study, with one lasting for more than one year and the other exhibiting an ongoing PFS for 6 months. Generally, liposarcoma, especially well-differentiated and dedifferentiated liposarcoma, is insensitive to systemic chemotherapy, and no standard treatment was recommended for recurrent liposarcoma after failure of doxorubicin-based chemotherapy.[35] It is reported that liposarcoma has some unique immune profile features, such as a higher proportion of tumor-infiltrating T cells and PD-L1 expression and more macrophage infiltration, compared with other STSs,[36] suggesting that immunotherapy could be an alternative therapeutic option for liposarcoma. Indeed, liposarcoma was one of the sarcoma subtypes that responded to anti-PD-1 antibody immunotherapy as reported in the SARC028 study.[6] Collectively, these studies suggest that liposarcoma may be another dominant sarcoma subtype in the clinical trial of TCR-T cell immunotherapy.

Clinical efficacy was corroborated by swift and robust expansions of TAEST16001 cells, as indicated by pharmacokinetic data from PCR. Moreover, continued expression of the TCR was observed up to 9 months post-infusion in some of the patients, suggesting the long-term persistence of TAEST16001 cells *in vivo*. In consistent with the long-term persistence of TAEST16001 cells *in vivo*, the duration of response in some patients last long as well in the current study. Similar to observations by D'Angelo et al.,[14] the frequency of T_{CM} subsets within the circulating TCR-T cells was increased with the extension of cell infusion, and this subset became the predominant cell subset on day 180–270 after cell infusion, which also in part explained the long persistence of TCR-T cells in the peripheral blood in our study. Although there was no statistically significantly difference in the peak of TCR gene copies among the four dosage levels, a relatively poor tumor response rate was observed at dose levels 2 and 3, which could be associated with a slow expansion of TCR *in vivo*. A special example was observed in patient T04, for whom the time to reach peak TCR-T cells was 1 h after cell infusion, suggesting that TCR-T cells did not proliferate *in vivo.* Correspondingly, a short stable disease was observed in patient T04. Our results did not show a positive correlation between the peak expansion of the TCR-T cells and tumor response, which may be due to the small sample size, and further investigation is warranted in the phase 2 study. All these results reveal that the magnitude and persistence of TCR-T cell expansion may be related to clinical efficacy.

The clinical efficacy of TAEST16001 cells was further verified by the higher amount of CRP and IFN-γ as observed in responders compared with that in nonresponders. Their increase suggested T cell activation, in line with previous reports.[37,38] IFN-γ has always been regarded as a key role in the activation of cellular immunity and the stimulation of anti-tumor response. Nowadays, pro- and anti-tumor effects of IFN-γ have been found; however, patients treated with high levels of IFN-γ had tumor regression.[39] Interestingly, the percentage of $CXCR3^+$ $CD3^+$ or $CXCR3^+CD3^+CD8^+$ T cells was statistically significantly increased in the responder group in our study, as IFN-γ is an essential factor associated with the induction of CXCR3 on T cells.[40] These results suggest that more $CXCR3^+CD8^+$ T cells in peripheral blood means more T cells trafficking to the tumor microenvironment and exhibiting stronger anti-tumor immune responses,[40] but this could not be evaluated in this study due to lack of available tumor samples.

In conclusion, data from this phase 1 clinical trial showed that autologous T cells engineered to express a high-affinity NY-ESO-1-specific TCR derived from PBMCs of an HLA-matched healthy donor are safe and highly active in the HLA-A*02:01 population with advanced STS expressing NY-ESO-1 antigens. A dose-reduced lymphodepletion with fludarabine and

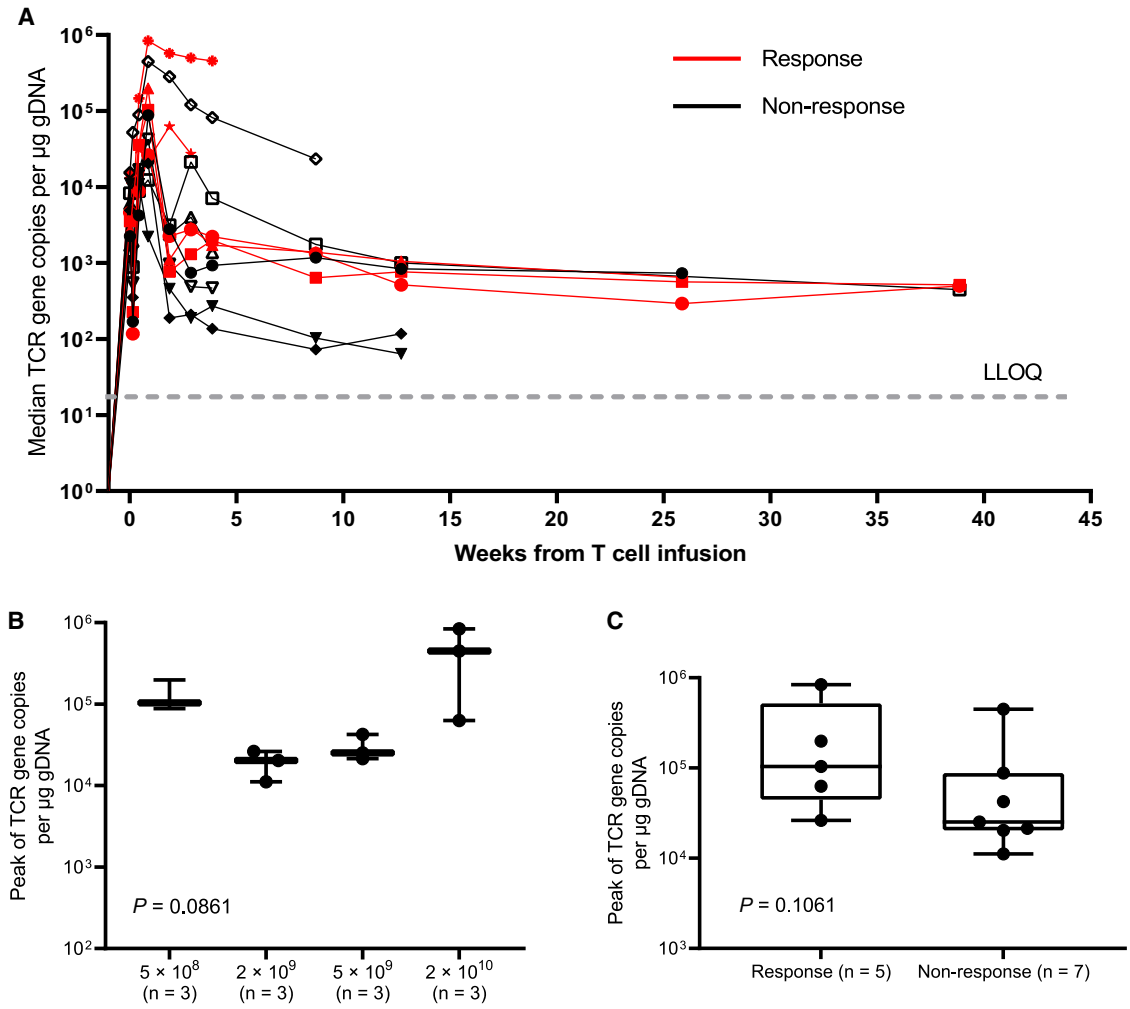

Figure 3. Peak TCR-engineered T cell expansion and association with response

(A) TCR copies as measured by vector transgene copies per µg genomic DNA in peripheral blood, according to clinical response. LLOQ, lower limit of quantitation.

(B) Peak TCR-engineered T cells levels by dose level.

(C) Association between peak TCR-engineered T cell expansion and the occurrence of tumor response. The horizontal lines within each box represent the median, the lower and upper borders of each box represent the interquartile range, and the bars show the range.

cyclophosphamide and low-dose IL-2 usage could minimize toxicity without decreasing efficacy. An expansion and phase 2 study of TAEST16001 cell treatment is ongoing to further assess the safety and clinical activity of the maximum escalating dose in patients with advanced soft tissue sarcoma. In addition, further investigation is needed to fully understand the long persistence of TAEST16001 cells and its association with patient responses.

Limitations of the study

Our study has several limitations. First, the major limitation was small sample size, so the association between peak TCR-T cell expansion *in vivo* and the infused cell dose should be further investigated. Second, biomarkers related to the response of the TCR-T cell treatment were not comprehensively understood, and more clinical validation is required.

STAR★METHODS

Detailed methods are provided in the online version of this paper and include the following:

- KEY RESOURCES TABLE
- RESOURCE AVAILABILITY
  - Lead contact
  - Materials availability
  - Data and code availability
- EXPERIMENTAL MODEL AND STUDY PARTICPANT DETAILS
  - Study design
  - Trial oversight
  - Eligibility
  - Treatment

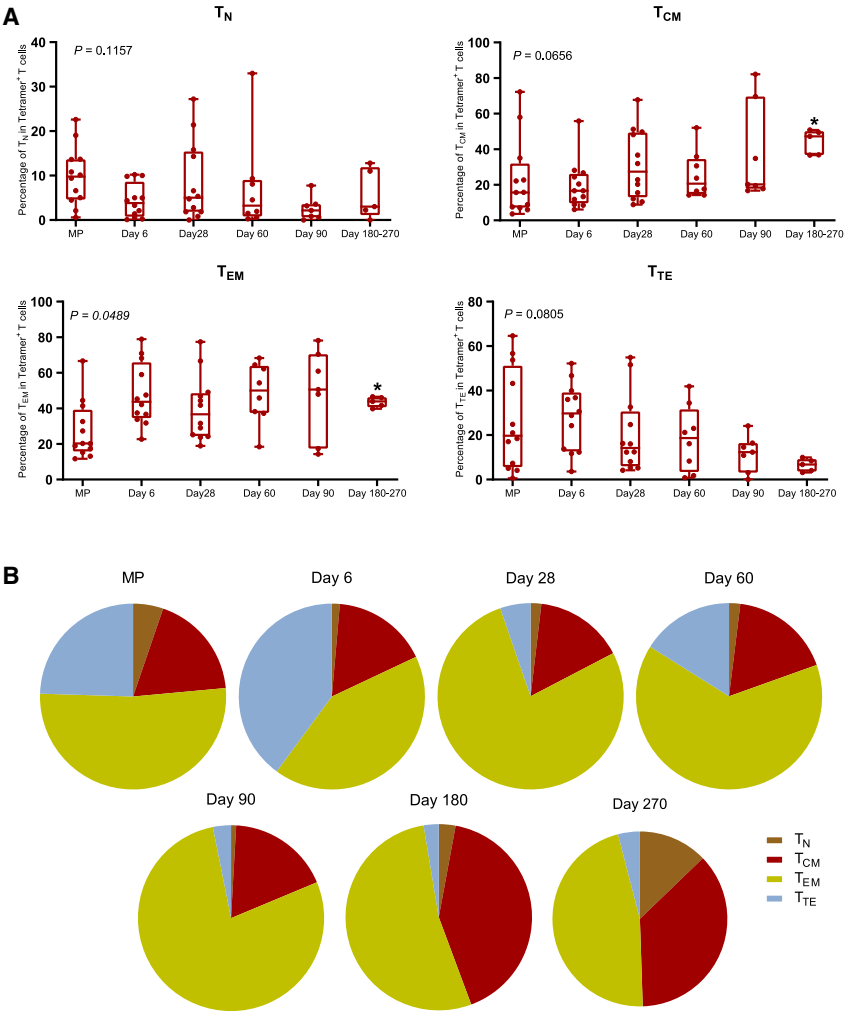

Figure 4. Phenotypic evolution of TAEST16001 cells and their correlation with the peak of TCR gene copies per μg gDNA after cell infusion

(A) The compositional evolution of TAEST16001 cell pool in peripheral blood. Naive T (T_N; $CD45RO^-$ $CCR7^+$) cells, central memory T (T_{CM}; $CD45RO^+$ $CCR7^+$) cells, effector memory T (T_{EM}; $CD45RO^+$ $CCR7^-$) cells, and terminally differentiated effector T (T_{TE}; $CD45RO^-CCR7^-$) cells were detected by flow cytometry in the manufactured product (MP) and at the time points indicated in each graph. The horizontal lines within each box represent the median, the lower and upper borders of each box represent the interquartile range, and the bars show the range. We calculated the p values using the Kruskal-Wallis (KW) test. *$p < 0.05$.

(B) Flow cytometry of tetramer-binding TAEST 16001 cells expressing CD45RO and CCR7 from patient T02 within the manufactured cell product (MP) and at the time points indicated in each graph after cell infusion. T_N cells, T_{CM} cells, T_{EM} cells, and T_{TE} cells were detected by flow cytometry.

(C) Correlation between frequencies of T cell subsets in the MP and the peak of TCR gene copies per μg gDNA after cell infusion. Spearman correlation analysis of the peak of TCR gene copies per μg gDNA after cell infusion and the frequencies of, T_{CM} ($CD45RO^+$ $CCR7^+$) cells, T_{EM} ($CD45RO^+CCR7^-$) cells, T_N ($CD45RO^-CCR7^+$) cells, and T_{TE}($CD45RO^-CCR7^-$) cells in TAEST16001 cell product.

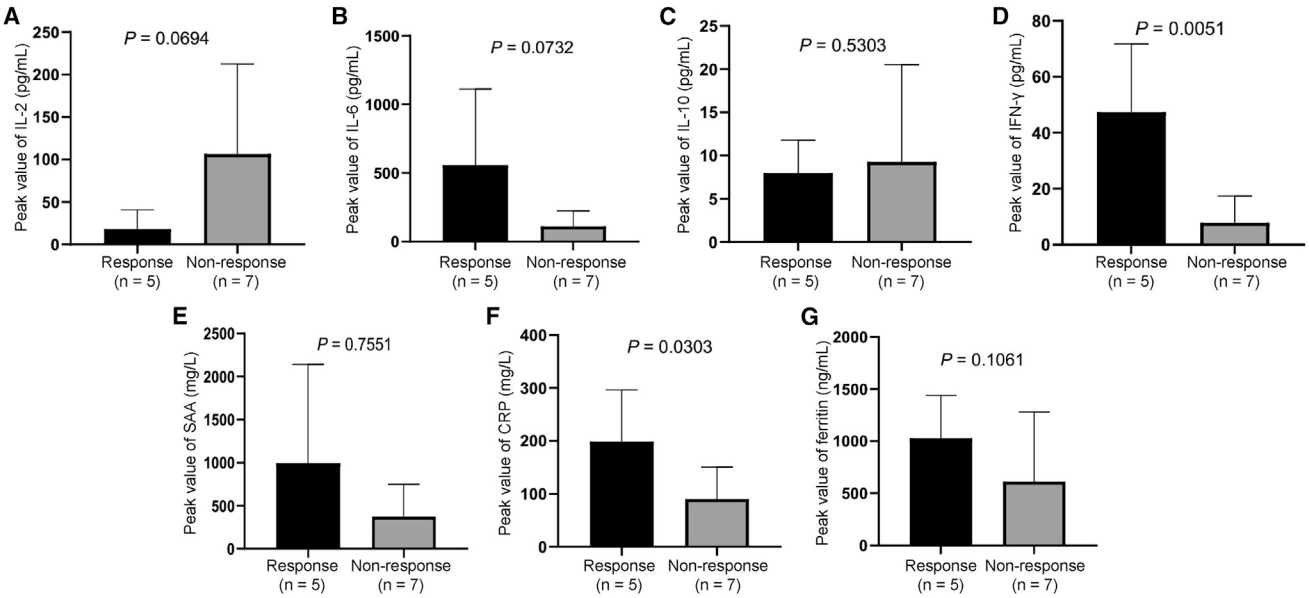

Figure 5. Associations between peak values of inflammatory cytokines and tumor response

(A–G) Relationship between (A) post-infusion interleukin-2 (IL-2) peak and treatment response; (B) post-infusion IL-6 peak and treatment response; (C) post-infusion IL-10 peak and treatment response; (D) post-infusion interferon-γ (IFN-γ) peak and treatment response; (E) post-infusion serum amyloid A (SAA) peak and treatment response; (F) post-infusion C-reactive protein (CRP) peak and treatment response; and (G) post-infusion ferritin peak and treatment response. Data are presented as mean ± SD. We calculated the p values using the two-sided Wilcoxon rank-sum test.

SUPPLEMENTAL INFORMATION

Supplemental information can be found online at https://doi.org/10.1016/j.xcrm.2023.101133.

ACKNOWLEDGMENTS

We thank patients and their families, as well as their caregivers, for taking part in this trial. This study was sponsored by Xiangxue Life Science Technology (Guangdong) Co., Ltd., the National Key Research and Development Program (2021YFC2400601), and the National Natural Science Foundation of China (82072958).

AUTHOR CONTRIBUTIONS

X.Z., Z.F., and Y. Li conceived and designed the study. D.W., Q.P., J.L., B.X., R.P., Y.Q., X.W., J.Y., Z.F., and X.Z. enrolled and treated patients. Y.O. was responsible for TCR-T cell product manufacturing. H.G. was responsible for TCR-T cell product quality. Y. Lin and K.M. did the immunological assay for cell product. Q.P., Y. Li, Z.H., S.Z., and X.Z. did exploratory immunological studies. Q.P. did the statistical analyses. Q.P., D.W., Z.H., L.Z., A.C., J.C., J.Y.N.L., J.L., Y. Li, Z.F., and X.Z. analyzed and interpreted the data. Q.P., Y. Li, and X.Z. wrote the manuscript. All authors reviewed the data, participated in the development of the manuscript, and approved the final version for publication.

DECLARATION OF INTERESTS

Z.H., Y.O., L.Z., H.G., A.C., J.C., S.Z., Y. Lin, Y. Li, and K.M. are employees of Xiangxue Life Science Technology (Guangdong) Co., Ltd.

Received: December 22, 2022
Revised: May 14, 2023
Accepted: July 7, 2023
Published: August 15, 2023

REFERENCES

1. von Mehren, M., Randall, R.L., Benjamin, R.S., Boles, S., Bui, M.M., Ganjoo, K.N., George, S., Gonzalez, R.J., Heslin, M.J., Kane, J.M., et al. (2018). Soft Tissue Sarcoma, Version 2.2018, NCCN Clinical Practice Guidelines in Oncology. J. Natl. Compr. Cancer Netw. *16*, 536–563. https://doi.org/10.6004/jnccn.2018.0025.
2. Li, R.H., Zhou, Q., Li, A.B., Zhang, H.Z., and Lin, Z.Q. (2020). A nomogram to predict metastasis of soft tissue sarcoma of the extremities. Medicine *99*, e20165. https://doi.org/10.1097/MD.0000000000020165.
3. Sleijfer, S., Ouali, M., van Glabbeke, M., Krarup-Hansen, A., Rodenhuis, S., Le Cesne, A., Hogendoorn, P.C.W., Verweij, J., and Blay, J.Y. (2010). Prognostic and predictive factors for outcome to first-line ifosfamide-containing chemotherapy for adult patients with advanced soft tissue sarcomas: an exploratory, retrospective analysis on large series from the European Organization for Research and Treatment of Cancer-Soft

Tissue and Bone Sarcoma Group (EORTC-STBSG). Eur. J. Cancer *46*, 72–83. https://doi.org/10.1016/j.ejca.2009.09.022.

4. Gronchi, A., Miah, A.B., Dei Tos, A.P., Abecassis, N., Bajpai, J., Bauer, S., Biagini, R., Bielack, S., Blay, J.Y., Bolle, S., et al. (2021). Soft tissue and visceral sarcomas: ESMO-EURACAN-GENTURIS Clinical Practice Guidelines for diagnosis, treatment and follow-up. Ann. Oncol. *32*, 1348–1365. https://doi.org/10.1016/j.annonc.2021.07.006.
5. Schöffski, P., Cornillie, J., Wozniak, A., Li, H., and Hompes, D. (2014). Soft tissue sarcoma: an update on systemic treatment options for patients with advanced disease. Oncol. Res. Treat. *37*, 355–362. https://doi.org/10.1159/000362631.
6. Tawbi, H.A., Burgess, M., Bolejack, V., Van Tine, B.A., Schuetze, S.M., Hu, J., D'Angelo, S., Attia, S., Riedel, R.F., Priebat, D.A., et al. (2017). Pembrolizumab in advanced soft-tissue sarcoma and bone sarcoma (SARC028): a multicentre, two-cohort, single-arm, open-label, phase 2 trial. Lancet Oncol. *18*, 1493–1501. https://doi.org/10.1016/S1470-2045(17)30624-1.
7. D'Angelo, S.P., Mahoney, M.R., Van Tine, B.A., Atkins, J., Milhem, M.M., Jahagirdar, B.N., Antonescu, C.R., Horvath, E., Tap, W.D., Schwartz, G.K., and Streicher, H. (2018). Nivolumab with or without ipilimumab treatment for metastatic sarcoma (Alliance A091401): two open-label, non-comparative, randomised, phase 2 trials. Lancet Oncol. *19*, 416–426. https://doi.org/10.1016/S1470-2045(18)30006-8.
8. Meyer, C.F. (2022). Immunotherapy for Sarcoma: A Work in Progress. J. Clin. Oncol. *40*, 1267–1270. https://doi.org/10.1200/JCO.21.01338.
9. Rizvi, H., Sanchez-Vega, F., La, K., Chatila, W., Jonsson, P., Halpenny, D., Plodkowski, A., Long, N., Sauter, J.L., Rekhtman, N., et al. (2018). Molecular Determinants of Response to Anti-Programmed Cell Death (PD)-1 and Anti-Programmed Death-Ligand 1 (PD-L1) Blockade in Patients With Non-Small-Cell Lung Cancer Profiled With Targeted Next-Generation Sequencing. J. Clin. Oncol. *36*, 633–641. https://doi.org/10.1200/JCO.2017.75.3384.
10. Pollack, S.M., He, Q., Yearley, J.H., Emerson, R., Vignali, M., Zhang, Y., Redman, M.W., Baker, K.K., Cooper, S., Donahue, B., et al. (2017). T-cell infiltration and clonality correlate with programmed cell death protein 1 and programmed death-ligand 1 expression in patients with soft tissue sarcomas. Cancer *123*, 3291–3304. https://doi.org/10.1002/cncr.30726.
11. Caballero, O.L., and Chen, Y.T. (2009). Cancer/testis (CT) antigens: potential targets for immunotherapy. Cancer Sci. *100*, 2014–2021. https://doi.org/10.1111/j.1349-7006.2009.01303.x.
12. Thomas, R., Al-Khadairi, G., Roelands, J., Hendrickx, W., Dermime, S., Bedognetti, D., and Decock, J. (2018). NY-ESO-1 Based Immunotherapy of Cancer: Current Perspectives. Front. Immunol. *9*, 947. https://doi.org/10.3389/fimmu.2018.00947.
13. Endo, M., de Graaff, M.A., Ingram, D.R., Lim, S., Lev, D.C., Briaire-de Bruijn, I.H., Somaiah, N., Bovée, J.V.M.G., Lazar, A.J., and Nielsen, T.O. (2015). NY-ESO-1 (CTAG1B) expression in mesenchymal tumors. Mod. Pathol. *28*, 587–595. https://doi.org/10.1038/modpathol.2014.155.
14. D'Angelo, S.P., Melchiori, L., Merchant, M.S., Bernstein, D., Glod, J., Kaplan, R., Grupp, S., Tap, W.D., Chagin, K., Binder, G.K., et al. (2018). Antitumor Activity Associated with Prolonged Persistence of Adoptively Transferred NY-ESO-1 (c259)T Cells in Synovial Sarcoma. Cancer Discov. *8*, 944–957. https://doi.org/10.1158/2159-8290.CD-17-1417.
15. Robbins, P.F., Kassim, S.H., Tran, T.L.N., Crystal, J.S., Morgan, R.A., Feldman, S.A., Yang, J.C., Dudley, M.E., Wunderlich, J.R., Sherry, R.M., et al. (2015). A pilot trial using lymphocytes genetically engineered with an NY-ESO-1-reactive T-cell receptor: long-term follow-up and correlates with response. Clin. Cancer Res. *21*, 1019–1027. https://doi.org/10.1158/1078-0432.CCR-14-2708.
16. Ramachandran, I., Lowther, D.E., Dryer-Minnerly, R., Wang, R., Fayngerts, S., Nunez, D., Betts, G., Bath, N., Tipping, A.J., Melchiori, L., et al. (2019). Systemic and local immunity following adoptive transfer of NY-ESO-1 SPEAR T cells in synovial sarcoma. J. Immunother. Cancer *7*, 276. https://doi.org/10.1186/s40425-019-0762-2.
17. Robbins, P.F., Morgan, R.A., Feldman, S.A., Yang, J.C., Sherry, R.M., Dudley, M.E., Wunderlich, J.R., Nahvi, A.V., Helman, L.J., Mackall, C.L., et al. (2011). Tumor regression in patients with metastatic synovial cell sarcoma and melanoma using genetically engineered lymphocytes reactive with NY-ESO-1. J. Clin. Oncol. *29*, 917–924. https://doi.org/10.1200/JCO.2010.32.2537.
18. Ishihara, M., Kitano, S., Kageyama, S., Miyahara, Y., Yamamoto, N., Kato, H., Mishima, H., Hattori, H., Funakoshi, T., Kojima, T., et al. (2022). NY-ESO-1-specific redirected T cells with endogenous TCR knockdown mediate tumor response and cytokine release syndrome. J. Immunother. Cancer *10*, e003811. https://doi.org/10.1136/jitc-2021-003811.
19. Liu, Q., Tian, Y., Li, Y., Zhang, W., Cai, W., Liu, Y., Ren, Y., Liang, Z., Zhou, P., Zhang, Y., et al. (2020). In vivo therapeutic effects of affinity-improved-TCR engineered T-cells on HBV-related hepatocellular carcinoma. J. Immunother. Cancer *8*, e001748. https://doi.org/10.1136/jitc-2020-001748.
20. Li, Y., Moysey, R., Molloy, P.E., Vuidepot, A.L., Mahon, T., Baston, E., Dunn, S., Liddy, N., Jacob, J., Jakobsen, B.K., and Boulter, J.M. (2005). Directed evolution of human T-cell receptors with picomolar affinities by phage display. Nat. Biotechnol. *23*, 349–354. https://doi.org/10.1038/nbt1070.
21. Zhang, H., Zhang, J., Chen, L., Weng, Z., Tian, Y., Zhao, H., Li, Y., Chen, L., Liang, Z., Zheng, H., et al. (2017). Targeting naturally occurring epitope variants of hepatitis C virus with high-affinity T-cell receptors. J. Gen. Virol. *98*, 374–384. https://doi.org/10.1099/jgv.0.000656.
22. Li, Z., Gong, H., Liu, Q., Wu, W., Cheng, J., Mei, Y., Chen, Y., Zheng, H., Yu, X., Zhong, S., and Li, Y. (2020). Identification of an HLA-A*24:02-restricted alpha-fetoprotein signal peptide-derived antigen and its specific T-cell receptor for T-cell immunotherapy. Immunology *159*, 384–392. https://doi.org/10.1111/imm.13168.
23. Robbins, P.F., Li, Y.F., El-Gamil, M., Zhao, Y., Wargo, J.A., Zheng, Z., Xu, H., Morgan, R.A., Feldman, S.A., Johnson, L.A., et al. (2008). Single and dual amino acid substitutions in TCR CDRs can enhance antigen-specific T cell functions. J. Immunol. *180*, 6116–6131. https://doi.org/10.4049/jimmunol.180.9.6116.
24. Nowicki, T.S., Berent-Maoz, B., Cheung-Lau, G., Huang, R.R., Wang, X., Tsoi, J., Kaplan-Lefko, P., Cabrera, P., Tran, J., Pang, J., et al. (2019). A Pilot Trial of the Combination of Transgenic NY-ESO-1-reactive Adoptive Cellular Therapy with Dendritic Cell Vaccination with or without Ipilimumab. Clin. Cancer Res. *25*, 2096–2108. https://doi.org/10.1158/1078-0432.CCR-18-3496.
25. Jones, H.F., Molvi, Z., Klatt, M.G., Dao, T., and Scheinberg, D.A. (2020). Empirical and Rational Design of T Cell Receptor-Based Immunotherapies. Front. Immunol. *11*, 585385. https://doi.org/10.3389/fimmu.2020.585385.
26. D'Ippolito, E., Schober, K., Nauerth, M., and Busch, D.H. (2019). T cell engineering for adoptive T cell therapy: safety and receptor avidity. Cancer immunology, immunotherapy *68*, 1701–1712. https://doi.org/10.1007/s00262-019-02395-9.
27. Linette, G.P., Stadtmauer, E.A., Maus, M.V., Rapoport, A.P., Levine, B.L., Emery, L., Litzky, L., Bagg, A., Carreno, B.M., Cimino, P.J., et al. (2013). Cardiovascular toxicity and titin cross-reactivity of affinity-enhanced T cells in myeloma and melanoma. Blood *122*, 863–871. https://doi.org/10.1182/blood-2013-03-490565.
28. June, C.H. (2007). Adoptive T cell therapy for cancer in the clinic. J. Clin. Invest. *117*, 1466–1476. https://doi.org/10.1172/JCI32446.
29. Schubert, M.L., Schmitt, M., Wang, L., Ramos, C.A., Jordan, K., Müller-Tidow, C., and Dreger, P. (2021). Side-effect management of chimeric antigen receptor (CAR) T-cell therapy. Ann. Oncol. *32*, 34–48. https://doi.org/10.1016/j.annonc.2020.10.478.
30. Carrasco-Padilla, C., Hernaiz-Esteban, A., Álvarez-Vallina, L., Aguilar-Sopeña, O., and Roda-Navarro, P. (2022). Bispecific Antibody Format and the Organization of Immunological Synapses in T Cell-Redirecting

Strategies for Cancer Immunotherapy. Pharmaceutics *15*, 132. https://doi.org/10.3390/pharmaceutics15010132.

31. Sharma, P., Hu-Lieskovan, S., Wargo, J.A., and Ribas, A. (2017). Primary, Adaptive, and Acquired Resistance to Cancer Immunotherapy. Cell *168*, 707–723. https://doi.org/10.1016/j.cell.2017.01.017.

32. Parkhurst, M.R., Yang, J.C., Langan, R.C., Dudley, M.E., Nathan, D.A.N., Feldman, S.A., Davis, J.L., Morgan, R.A., Merino, M.J., Sherry, R.M., et al. (2011). T cells targeting carcinoembryonic antigen can mediate regression of metastatic colorectal cancer but induce severe transient colitis. Mol. Ther. *19*, 620–626. https://doi.org/10.1038/mt.2010.272.

33. Tucker, C.G., Mitchell, J.S., Martinov, T., Burbach, B.J., Beura, L.K., Wilson, J.C., Dwyer, A.J., Singh, L.M., Mescher, M.F., and Fife, B.T. (2020). Adoptive T Cell Therapy with IL-12-Preconditioned Low-Avidity T Cells Prevents Exhaustion and Results in Enhanced T Cell Activation, Enhanced Tumor Clearance, and Decreased Risk for Autoimmunity. J. Immunol. *205*, 1449–1460. https://doi.org/10.4049/jimmunol.2000007.

34. McLane, L.M., Abdel-Hakeem, M.S., and Wherry, E.J. (2019). CD8 T Cell Exhaustion During Chronic Viral Infection and Cancer. Annu. Rev. Immunol. *37*, 457–495. https://doi.org/10.1146/annurev-immunol-041015-055318.

35. Crago, A.M., and Dickson, M.A. (2016). Liposarcoma: Multimodality Management and Future Targeted Therapies. Surg. Oncol. Clin. *25*, 761–773. https://doi.org/10.1016/j.soc.2016.05.007.

36. Roulleaux Dugage, M., Nassif, E.F., Italiano, A., and Bahleda, R. (2021). Improving Immunotherapy Efficacy in Soft-Tissue Sarcomas: A Biomarker Driven and Histotype Tailored Review. Front. Immunol. *12*, 775761. https://doi.org/10.3389/fimmu.2021.775761.

37. Qi, C., Gong, J., Li, J., Liu, D., Qin, Y., Ge, S., Zhang, M., Peng, Z., Zhou, J., Cao, Y., et al. (2022). Claudin18.2-specific CAR T cells in gastrointestinal cancers: phase 1 trial interim results. Nat. Med. *28*, 1189–1198. https://doi.org/10.1038/s41591-022-01800-8.

38. Zhou, Z.Q., Zhao, J.J., Pan, Q.Z., Chen, C.L., Liu, Y., Tang, Y., Zhu, Q., Weng, D.S., and Xia, J.C. (2019). PD-L1 expression is a predictive biomarker for CIK cell-based immunotherapy in postoperative patients with breast cancer. J. Immunother. Cancer *7*, 228. https://doi.org/10.1186/s40425-019-0696-8.

39. Jorgovanovic, D., Song, M., Wang, L., and Zhang, Y. (2020). Roles of IFN-gamma in tumor progression and regression: a review. Biomark. Res. *8*, 49. https://doi.org/10.1186/s40364-020-00228-x.

40. Groom, J.R., and Luster, A.D. (2011). CXCR3 in T cell function. Exp. Cell Res. *317*, 620–631. https://doi.org/10.1016/j.yexcr.2010.12.017.

41. Lee, D.W., Santomasso, B.D., Locke, F.L., Ghobadi, A., Turtle, C.J., Brudno, J.N., Maus, M.V., Park, J.H., Mead, E., Pavletic, S., et al. (2019). ASTCT Consensus Grading for Cytokine Release Syndrome and Neurologic Toxicity Associated with Immune Effector Cells. Biol. Blood Marrow Transplant. *25*, 625–638. https://doi.org/10.1016/j.bbmt.2018.12.758.

STAR★METHODS

KEY RESOURCES TABLE

REAGENT or RESOURCE	SOURCE	IDENTIFIER
Antibodies		
Anti-CD3 APC	Biolegend	Cat# 317318; RRID: AB_1937212
Anti-CD3 BV510	BD biosciences	Cat# 564713; RRID: AB_2738909
Anti-CD4 BUV496	BD biosciences	Cat# 564651; RRID: AB_2744422
Anti-CD8 APC-Cy7	Biolegend	Cat# 300926; RRID: AB_10613636
Anti-CD45 AF700	Biolegend	Cat# 304024; RRID: AB_493761
Anti-CCR7 BV421	Biolegend	Cat# 353208; RRID: AB_11203894
CCR7-FITC	Biolegend	Cat# 353216; RRID: AB_10916386
CD45RO-BV421	Biolegend	Cat# 304224; RRID: AB_2563817
Anti-CD45RO BV605	BD biosciences	Cat# 562791; RRID: AB_2744411
Anti-CD25 BUV737	BD biosciences	Cat# 612806; RRID: AB_2870132
Anti-CXCR6 BV421	BD biosciences	Cat# 566007; RRID: AB_2744472
Anti-CXCR3 BV605	Biolegend	Cat# 353728; RRID: AB_2563157
Anti-Tim-3 BV711	BD biosciences	Cat# 565566; RRID: AB_2744370
Anti-CTLA-4 PE	Biolegend	Cat# 349906; RRID: AB_10641842
Anti-LAG-3 PE-Cy7	eBioscience	Cat# 25-2239-42; RRID: AB_2573430
Anti-PD-1 PerCP-Cy5.5	Biolegend	Cat# 329914; RRID: AB_1595461
Anti-Foxp3 AF488	Biolegend	Cat# 320112; RRID: AB_430883
Biological samples		
Leukopak	Milestone Biotechnologies	Cat# PBLP-F-3
Chemicals, peptides, and recombinant proteins		
Peptides	Genscript	Cat# SC1208
Tetramer	This manuscript	N/A
Recombinant Human Il-2	Beijing Four Rings Biopharmaceuticals Co., Ltd.	Cat# S20040018
DEPC-H2O	Invitrogen	Cat # 750023
Buffer TE	Invitrogen	Cat # AM9849
Ethanol (96–100%)	Sinopharm	Cat # 10009259
HIV-Psi F	GENEWIZ	NA
HIV-Psi R	GENEWIZ	NA
HIV-Psi Probe	GENEWIZ	NA
XL-1901	Provided by sponsor	Cat # XL-1901 ps190820
RCLVSVG F	GENEWIZ	NA
RCLVSVG R	GENEWIZ	NA
RCLVSVG Probe	GENEWIZ	NA
pMD2.G	Provided by sponsor	Cat # ps19010901
Human Fc block	BD	Cat#564220
Staining Buffer	Biolegend	Cat#420201
Brilliant Stain Buffer	BD	Cat#566349
IC fixation buffer	BD	Cat#554655
RBC lysing solution	BD	Cat#555899
PIC	Genescript	customized
P72A	Genescript	7195038–1
RPMI-1640	Gibco	Cat # A1049101
FBS	ExCell	FSP500

(*Continued on next page*)

Continued

REAGENT or RESOURCE	SOURCE	IDENTIFIER
Critical commercial assays		
CytoTox 96® non-radioactive cytotoxicity assay kit	Promega	Cat# G1780
Human IFN-γ ELISpot Set	BD biosciences	Cat# 551849
V-PLEX Custom Human Cytokine Panel	MSD	Cat# K151A0H-1
Proinflammatory panel 1 (human) control pack	MSD	Cat# C4049-1
Chemokine panel 1(human) control pack	MSD	Cat# C4047-1
Cytokine panel 1(human) control pack	MSD	Cat# C4050-1
QIAamp DNA Blood Midi Kit	Qiagen	Cat# 51183 or 51185
Faststart Universal Probe Master	Roche	Cat# 04914058001
CD14 Microbeads	Miltenyi	Cat# 272-01
CD25 Microbeads	Miltenyi	Cat# 274-01
Dynabeads CD3/CD28 CTS	ThermoFisher	Cat# 40203D
QIAamp DNA Blood Midi Kit	Qiagen	Cat # 51185
FastStart Universal Probe Master	Roche	Cat # 04914058001
V-PLEX Custom Human Cytokine panel	Meso Scale Discovery	Cat # MSD-K151A9H-1
Proinflammatory panel 1(human) control pack	Meso Scale Discovery	Cat #C4049-1
Chemokine panel 1 (human) control pack	Meso Scale Discovery	Cat #C4047-1
Cytokine panel 1 (human) control pack	Meso Scale Discovery	Cat #C4050-1
LIVE/DEAD™ Fixable Red Dead Cell Stain Kit	eBioscience	Cat#L34972
Foxp3/Transcription Factor Staining Buffer Set (contain Fix/Perm buffer, Perm/Wash buffer)	eBioscience	Cat#00-5523-00
Human IFN-γ ELISpot PLUS kit (ALP)	Mabtech	Cat # 3420-4AST-10
Experimental models: Cell lines		
A375	ATCC	Cat# CRL-1619
IM9	ATCC	Cat# CCL-159
U266B1	ATCC	Cat# TIB-196
T2	ATCC	Cat# CRL-1992
NCI-H1650	ATCC	Cat# CRL-5883
NCI-H1703	ATCC	Cat# CRL-5889
NCI-H1299	ATCC	Cat# CRL-5803
SW480	ATCC	Cat# CCL-228
Software and algorithms		
Statistical Package for the Social Science, version 22.0	IBM Corp	N/A
GraphPad Prism 9	GraphPad Software, Inc.	N/A
cytExpert, version 2.0	Beckman Coulter	N/A
FlowJo software, Version 10	BD	NA

RESOURCE AVAILABILITY

Lead contact

Further information and requests for resources and reagents should be directed to and will be fulfilled by the lead contact, Xing Zhang (zhangxing@sysucc.org.cn).

Materials availability

This study did not generate new unique reagents.

Data and code availability

Data from this study can be made available upon request and approval by the study management committee and subject to appropriate data transfer agreements. Requests should be directed to X.Z. No custom code was used for statistical analysis for this study. Any additional information required to reanalyze the data reported in this work paper is available from the lead contact upon request.

EXPERIMENTAL MODEL AND STUDY PARTICPANT DETAILS

Study design

This study was an open-label, single-arm phase 1 study, with a conventional 3 + 3 dose escalation/expansion design. Four dose levels were planned: dose level 1, $5 \times 10^8 \pm 30\%$; dose level 2, $2 \times 10^9 \pm 30\%$; dose level 3, $5 \times 10^9 \pm 30\%$; and dose level 4, $1.2 \times 10^{10} \pm 30\%$. Starting doses were based on previous studies,[15,17] in which the number of infused TCR-T cells was between 3.5×10^8 and 2.9×10^{10}. At least three patients per dose cohort were recruited and no dose-limiting toxic (DLT) effect was observed during a 28-day observation period before dose escalation. If a DLT was recorded, three more patients were recruited to the cohort in which the DLT occurred. Intrapatient dose escalation was not allowed. The MTD was defined as the highest dose at which one or fewer of six patients had a DLT after cell infusion.

Trial oversight

The study was approved by the Institutional Review Board of Sun Yat-sen University Cancer Center, conducted according to the principles of the Declaration of Helsinki, and was registered on ClinicalTrials.gov (NCT04318964). All patients provided written informed consent before enrollment.

Eligibility

Patients were eligible if they were aged 18 through 70 years; had HLA-A*02:01 allele and $\geq$20% of tumor cells expressing the NY-ESO-1 tumor antigen by immunohistochemistry; had histologically confirmed advanced soft tissue sarcoma that was unresectable, metastatic, or refractory to standard treatments; have at least 1 measurable disease by Computed Tomography (CT) or Magnetic Resonance (MR) scans (per Response Evaluation Criteria In Solid Tumors [RECIST] v1.1); had an Eastern Cooperative Oncology Group performance status score of 0 or 1; had a life expectancy of at least 3 months; had left ventricular ejection fraction of $\geq$50%; and had adequate liver, kidney, and bone marrow function.

Key exclusion criteria included: anticancer therapy within 4 weeks of cell infusion; history of NY-ESO-1-targeted therapy; concomitant corticosteroids, or immunomodulatory drugs within 4 weeks of cell infusion; history of brain metastases or active infection or other uncontrolled significant medical or psychiatric illness; and history of autoimmune diseases.

Treatment

After TAEST16001 cells were successfully manufactured and met the quality control, patients received a modified lymphodepleting regimen of intravenous fludarabine 20 mg/m^2 per day and cyclophosphamide 15 mg/kg per day for 3 consecutive days beginning on day -7 before cell infusion. On day 1, the full dosage of TAEST16001 cells was administered intravenously over 30 min once (at dose level 1 or 2) or twice in two consecutive days (at dose level 3 or 4). IL-2 was subcutaneous injection within 30 min after the first cell infusion at a dose of 500,000 IU each time, twice daily for 14 days.

Clinical assessments

Peripheral blood samples were taken for safety, pharmacokinetic, and pharmacodynamic analyses during the study period at predefined visit. Safety was assessed by means of adverse event monitoring, graded according to the NCI Common Terminology Criteria for Adverse Events v5.0. Cytokine release syndrome (CRS) and immune effector cell–associated neurotoxicity syndrome (ICANS) were graded according to the ASTCT 2018 guideline.[41] DLTs were defined as adverse events occurred within 28 days of the TAEST16001 cell infusion judged possibly related to the cell infusion. Non-haematological DLTs were any toxicity of grade 3 persisted for seven or more days or any toxicity of grade 4 regardless of duration, with exceptions detailed in the study protocol (Methods S1). Haematological DLTs were grade 4 toxicity (except lymphopenia) lasting more than 28 days if not due to underlying disease. Grade 3 CRS lasting more than 7 days or grade 4 CRS was also considered as DLT. The parameters related with pharmacokinetic and pharmacodynamic analyses were provided by Immunology Center WuXi AppTec in Shanghai, China.

Tumors were assessed by CT or MR scans performed at baseline and on day 28, day 60, day 90, day 180, and day 270 after TAEST16001 cell infusion. Tumor response was evaluated by the RECIST v1.1. Patients who were evaluated as progressive disease (PD) by RECIST v1.1 could be re-evaluated as immune unconfirmed PD (iUPD) according to the immune Response Evaluation Criteria In Solid Tumors (iRECIST) and re-assessed after 4–6 weeks until immune confirmed progressive disease (iCPD) or initiating other anti-tumor treatment, whichever occur first.

The primary objectives were to investigate the safety, tolerability, and DLTs of TAEST16001 cells to identify the MTD. Safety endpoints included adverse events, serious adverse events, adverse events of special interest (CRS and ICANS), laboratory tests, physical examination assessments, electrocardiogram, and vital sign measurements.

The secondary objectives were pharmacokinetics, pharmacodynamics, objective response rate (ORR, the proportion of patients who achieved a RECIST 1.1 confirmed complete response or partial response), disease control rate (DCR, the proportion of patients who reached an objective response or stable disease), and PFS (the number of days between patients' enrollment and either disease progression or death after cell infusion). For pharmacokinetics analyses, TAEST16001 cells as well as the TCR gene copies per μg genomic DNA (gDNA) were detected by flow cytometry and qPCR, respectively, to calculate the maximum value of TCR-T cells in

peripheral blood (C_{max}) and the time to reach peak concentration (T_{max}). For pharmacodynamics analyses, T cell subsets and antigen-specific cytotoxic T lymphocytes in peripheral blood were detected.

We also assessed correlations between response and selected prespecified biomarkers: TCR gene copies per μg gDNA, inflammatory cytokines (IL-2, IL-6, IL-10, interferon-γ (IFN-γ), Serum amyloid A (SAA), C-reactive protein (CRP), and ferritin).

METHOD DETAILS

NY-ESO-1 expression

NY-ESO-1 antigen was tested by immunostaining at the Sun Yat-sen University Cancer Center. Immunohistochemistry (IHC) was carried out using primary antibody against NY-ESO-1 on 3∼5-mm-thick sections of formalin-fixed, paraffin-embedded tumor tissue sections. Then, the sections were visualized by DAB and counterstained with hematoxylin as per the manufacturer's instructions. More than 20% of tumor cells expressing the NY-ESO-1 tumor antigen by IHC were defined as NY-ESO-1 positive expression in the study.

The full TCR sequence

atggagacactgctgggcgtgagcctggtcatcctgtggctccagctggcccgggtgaacagccagcagggagaggaggacccccaggccctgagcatccaggagggcgag
aatgccaccatgaactgctcctacaagacatccatcaacaacctccagtggtatcggcagaacagcggccggggcctggtgcacctgatcctgatcaggtctaacgagaggg
agaagcacagcggccggctgagagtgaccctggacacaagcaagaagagctcctctctgctgatcaccgcctccagagccgccgatacagcctcttacttttgcatgtatgac
cagaacggcaagatcatcttcggcaagggcaccaggctgcacatcctgcctaatatccagaacccagatcccgccgtgtaccagctgcgcgacagcaagagctccgataaga
gcgtgtgcctgttcaccgactttgattcccagacaaacgtgagccagtctaaggactctgacgtgtacatcaccgacaagacagtgctggatatgaggagcatggactttaagagc
aattccgccgtggcctggtctaacaagagcgacttcgcctgcgccaacgcctttaacaatagcatcatcccagaggataccttcttttgctccccagagtctagctgtgacgtgaa
gctggtggagaagagcttcgagacagatacaaatctgaactttcagaatctgtccgtgatcggcttcagaatcctgctgctgaaggtggccggctttaacctgctgatgaccctga
gactgtggtcctctggctctcgggccaagagatctggcagcggcgccacaaatttcagcctgctgaagcaggcaggcgatgtggaggagaacccaggacctagagacagct
ggaccctgtgctgcgtgagcctgtgcatcctggtggccaagcacacagacgccggcgtgatccagtctccacggcacgaggtgaccgagatgggccaggaggtgacactg
aggtgtaagcccatcagcggccacgattacctgttttggtataggcagaccatgatgcgcggcctggagctgctgatctacttcaacaataacgtgcccatcgacgattctggc
atgcctgaggaccggtttagcgccaagatgccaaatgcctccttctctaccctgaagatccagccttctgagccaagagatagcgccgtgtacttttgcgccagctccctggg
ctccaatgagcagtatttcggccccggcacaaggctgaccgtgacagaggacctgaagaacgtgttcccccctgaggtggccgtgtttgagccttccgagtgcgagatctctca
cacccagaaggccaccctggtgtgcctggcaaccggcttctatccagatcacgtggagctgagctggtgggtgaatggcaaggaggtgcactccggcgtgtctacagacccaca
gcccctgaaggagcagcccgccctgaacgattcccgctactgcctgtctagcaggctgcgcgtgtctgccacctttggcagaatcctcggaaccacttcagatgtcaggtgcagtt
ttatggcctgagcgagaacgatgagtggacccaggacagggccaagcctgtgacacagatcgtgtccgccgaggcctggggaagggcagactgtggcttcacaagcgagtccta
ccagcagggcgtgctgtccgccaccatcctgtacgagatcctgctgggcaaggccacactgtatgccgtgctggtgtccgccctggtgctgatggccatggtgaagaggaagga
ttctcgcggctga.

Generation of TAEST16001 cells

Patients underwent leukapheresis at enrollment to collect peripheral blood mononuclear cells (PBMCs). High-affinity NY-ESO-1-specific TCR-T cells (TAEST16001 cells) were manufactured at Xiangxue Life Science Technology (Guangdong) Co., Ltd. TAEST16001 cells were generated from $CD14^{-}$and CD25-depleted PBMCs by Sepax C-pro and CliniMACS plus. CD14 and CD25 negative cells were activated and expanded using αCD3/αCD28 antibody-conjugated beads in the presence of 200 IU/mL of recombinant IL-2, transduced with a lentivirus at a multiplicity of infection of 1 transducing unit per cell. Cells were expanded for 9–13 days by Wave Bioreactor and then harvested by Sefia and formulated by Sepax C-pro. TCR-T cell product would be frozen for release testing, which took an additional 7–10 days. So far, the manufacture process works well and no manufacturing failures occurred.

qPCR analysis of TAEST16001 cell expansion and persistence

TCR gene copies per microgram of gDNA were determined at the Immunology Center WuXi AppTec by quantification of the WPRE region of the lentivirus backbone by qPCR. 6 mL peripheral blood samples were taken at baseline and after infusion. Genomic DNA was extracted from PBMCs using the QIAamp DNA Blood Midi Kit (Qiagen). A series dilution of a plasmid was used to prepare a standard curve with a high, middle and low controls. 5 μL gDNA and standard were amplified with Quant Studio 7 Flex Real-Time PCR System (Thermo Fisher Applied Biosystems) using the respective primers, probes and FastStart Universal Probe Master Mix. The number of TCR gene copies per microgram of gDNA was determined triplicated for each sample. The limit of detection for this assay was 20 copies per microgram of gDNA.

RCL discovery by using TaqMan Real-time PCR

TaqMan qPCR was used to determine the RCL. A dilution series of a plasmid was used to prepare standard curve with high, middle and low controls. gDNA were extracted from ∼2 mL whole blood using QIAamp DNA Blood Midi Kit. 5 μL gDNA and standard were amplified with Quant Studio 7 Flex Real-Time PCR System (Thermo Fisher Applied Biosystems) using the respective primers, probes and FastStart Universal Probe Master Mix.

Cytokine measurement

Human serum was used to detect human cytokine/chemokine/proinflammatory. The MSD V-PLEX Plus Custom Human Biomarkers Kit from MSD was used to measure IL-2, IL-6, IL-10, and IFN-γ. MSD plates were analyzed on the MESO SECTOR S600. The assay was performed following the manufacturer's instructions. All standards, controls and samples were measured in duplicate.

Flow cytometry

Whole blood samples were collected with heparin vacuum tube (BD) and processed with RBC lysis buffer to remove red blood cell. Multi-parametric immune-phenotyping for peripheral blood was performed using approximately 1.0×10^6 total cells per condition (depending on cell yield in samples), and using isotype stains in PK analysis. Cells were stained in staining buffer for 45 min at room temperature using antibody and reagent concentrations recommended by the manufacturer. PK samples were stained with A2P1B, anti-CD45, CD3, CD4 and CD8 antibodies, PD samples were stained with A2P1B, anti-CD45, CD3, CD4, CD8, CCR7, and CD45RO antibodies for Tet+ T cell subsets analysis; and were stained with A2P1B, anti-CD45, CD3, CD4, CD8, CD25, CXCR3, CXCR6, TIM-3, PD-1, CTLA-4 and LAG-3 antibodies, permeablized with Fix/Perm buffer for 30 min, and stained with anti-Foxp3 antibody for Treg analysis, respectively. Cells were then washed, and re-suspended in staining buffer and acquired using an BD Fortessa cytometer equipped with an Ultraviolet (355 nm), Violet (405 nm), Blue (488 nm), Yellow (561 nm) and Red (633 nm) laser. Flow cytometry files were exported in.fcs file format and analyzed using FlowJo software (Version 10, BD).

Peptides and tetramer

Peptides were synthesized (>95% purity) by GenScript and verified using mass spectroscopy. MHC tetramers were produced in-house.

Human IFN-γ ELISpot assay

IFN-γ ELISpot were determined using the Human IFN-γ ELISpot Set (BD Biosciences). Human PBMCs were used to detect effector cell activity. IFN-γ ELISpot assay was performed using 96-well ELISpot strip plates (8 wells × 12 strips) pre-coated with monoclonal antibody. The assay was performed following the manufacturer's instructions. Plates were blocked with RPMI-1640 medium (0.2 mL/well) containing 10% FBS for at least 30 min at room temperature after washing 4 times with sterile DPBS (0.2 mL/well). 100 μL Peptide pools were added to the plate. Plate were incubated the at 37°C 5% CO_2 for 16 h without moving after adding the same volume cells. Plate was washed 5 times using PBS with a volume of 0.2 mL per well. Diluted detection antibody (R4-6A2-biotin) was added with a volume of 0.1 mL per well for 2 h at room temperature. After washing the plate 5 times with DPBS, diluted Streptavidin-ALP was added with a volume of 0.1 mL per well for 1 h. Plates were washed 5 times with PBS, and then substrate solution (BCIP/NBT-plus) were added with a volume of 0.1 mL per well. Plates were developed until distinct spots emerge and stopped color development by washing extensively in tap water. After the plates were dried, read the plates and analyzed the results by using AID ELISpot Software 7.0.

Quantification and statistical analysis

The sample size was based on the conventional 3 + 3 dose escalation/expansion design and the number of DLTs. We summarized the number of cases, median, interquartile range, minimum and maximum values for continuous variables and frequency distributions for categorical variables with descriptive statistics. We assessed the association between response and biomarkers as stated above with a Mann-Whitney U test. We evaluated the difference in the phenotype of TCR-T cells among different time with a Kruskal-Wallis (KW) test. We reported estimates of ORR and DCR with the corresponding two-sided exact binomial 95% CI, calculated by means of the Clopper-Pearson method. Kaplan-Meier method was used to estimate progression-free survival (PFS). We used SPSS software (Statistical Package for the Social Science, version 22.0, IBM Corp. Armonk, NY, USA) and GraphPad Prism 9 (Version 9.3.1, GraphPad Software, Inc.) for all analyses.

ADDITIONAL RESOURCES

This trial is registered with ClinicalTrials.gov, NCT04318964.